Small-Scale Solar Cogeneration Systems

A. Ryyan and G. Bastian

Abstract—**Solar cogeneration systems provide electrical energy as well as thermal energy. This combination is common in many large-scale solar power plants, but rare in small-scale domestic systems. We are introducing a combination of recent developments, which can overcome existing problems aiming at a medium temperature domestic system. Advanced non-imaging solar concentrators, thin-film thermoelectric modules and high temperature selective absorbers are promising techniques to achieve a non-tracking cogeneration system with reasonable cost and performance levels.**

Index Terms—**Cogeneration, solar, thermoelectrics.**

I. Introduction

One challenge for system designers is the conversion of one form of energy into another form of energy using the most efficient means. In particular, cogeneration systems can be considered to optimize the total efficiency, i.e. maximizing both electrical and heat output performance. During the last decades a large variety of photovoltaic (PV) cells with efficiencies η as high as 44.7% [1] has been developed for different fields of application. In contrast, solar heating systems are used either in large-scale power plants or for domestic water heating. Solar cogeneration systems with heat and electricity output are commonly based on two effects: Either the PV components are attached to heat exchangers such that they are cooled by water, or the solar spectrum is split into two fractions - the longer wavelengths are used for solar heating, the shorter wavelengths for PV.

Large-scale solar thermal power plants create heat at the highest temperatures possible, which is successively converted into mechanical energy and electrical energy with the help of some thermodynamic cycle, limited by the Carnot efficiency. In order to achieve the highest temperatures, different kinds of focusing techniques in combination of solar tracking devices are used.

The purpose of this paper is to evaluate to which extent small-scale solar non-tracking cogeneration systems are feasible. Several authors have suggested one-dimensional concentration and tubular absorber geometries [2]-[5]. Our optimization is considering two-dimensional reflector shapes, selective absorber coating spectra, and secondary heat conversion components. In the first section, we discuss the limits of solar concentration factors by using non-imaging optimized reflector designs. In the second section, we present calculation results on maximum absorber temperatures based on the achieved concentration factors. The resulting Carnot-efficiencies and optimized operation conditions are derived. The third section describes possible implementations into real systems and discusses suitable technologies for conversion into electrical power.

II. Light Concentration

Solar radiation can be concentrated using optical components by a factor of up to approximately c=1000 using parabolic dishes, large-scale Fresnel lenses or other kind of lenses [6] manufactured with high precision. Tracking of the solar irradiation angles is required as this concentration factor works only for a very small angle interval. In contrast to that, a system which accepts all irradiation angles offers no concentration at all, i.e. c=1. The theoretical maximum concentration factor [7] is determined by the acceptance angle interval $\Delta\varphi$:

$$c = \frac{1}{(\sin\Delta\varphi)^2} \tag{1}$$

As domestic solar systems are mounted onto roofs at different locations with different elevation and cardinal directions, often no concentration is considered. Only compound parabolic concentrators (CPC) as external one-dimensional reflectors are widely used – mainly in order to harvest diffusive light from all directions rather than for an enhanced concentration factor.

The solar elevation and azimuth angles do not cover a full range of $\pm\pi$, neither during the monthly nor the daily cycles. As such, restricted angle intervals can be considered in order to gain a concentration which is enhanced to some extent. Fig. 1 shows an example of how the irradiance angles change during each day and month for the location of Gaza, Palestine.

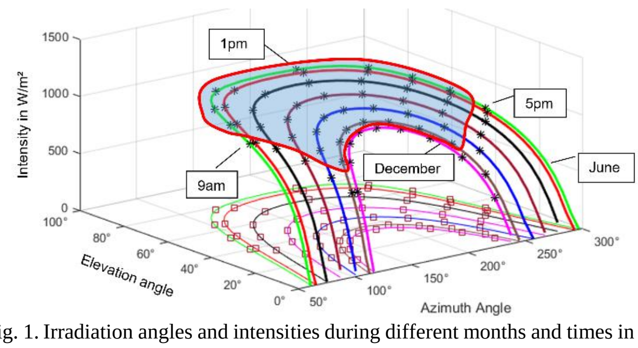

Fig. 1. Irradiation angles and intensities during different months and times in Gaza.

Along with different irradiation angles, the solar radiation experiences different air-masses (AM), which lead to a reduced solar intensity I as compared to the extraterrestrial intensity I_0 (after [8]):

$$I = 1.1 \cdot I_0 \cdot 0.7^{AM^{0.678}} \tag{2}$$

Manuscript received June 15, 2018; revised September 12, 2018.
Georg Bastian is with the Rhein-Waal University of Applied Sciences, Germany (e-mail: Georg.Bastian@hochschule-rhein-waal.de).

doi: 10.18178/jocet.2018.6.5.493

This intensity reduction along with each angle of incidence can be seen in Fig. 1. If the reflector optimization is limiting the azimuth angle, an improved solar concentration and increased temperatures can be achieved. Restrictions in the elevation and the azimuthal angles limit the high concentration and thus high temperature operations to fewer hours per day. Nevertheless, the total power conversion efficiency can be enhanced as it is limited by Carnot efficiency.

The simulation and optimization of the reflector shape was performed using FRED 15.90 Optimum ray tracing software [9].

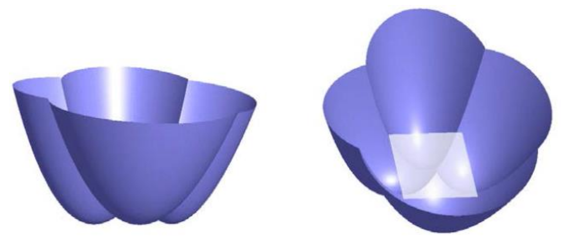

Fig. 2. The optimized 2D reflector shape (blue) and absorber area (white).

Suitable geometries, as shown in Fig. 2, were computed by considering all angles of incidence from January to November, 10am to 4pm, as indicated by the loop in Fig. 1. The reflector surface was described by a 2D parabolic approximation with a flat rectangular area as the absorbing surface.

Not all incident rays hit the absorbing plate, for different angles of incidence. The optical efficiency of the reflector is 52.9% with a concentration factor of 6.4, yielding an effective annual average concentration of c=3.38. This concentration factor varies for different months and times of the day, as shown in Table I.

TABLE I: VARIATION THE OPTICAL EFFICIENCY AND THE EFFECTIVE CONCENTRATION FACTOR AT DIFFERENT SOLAR IRRADIATION ANGLES

Time	Optical efficiency	Ratio of aperture vs. absorber area	Effective concentration factor
January 13:00	62.1%	6.4	3.98 c
January 10:00	10.7%	6.4	0.68
June 13:00	87.4%	6.4	5.59
June 10:00	20.0%	6.4	1.28
Annual average	52.9%	6.4	3.38

Depending on the cogeneration technique and the heat storage medium, different concentration factors and temperatures are preferred over others. The total duration of solar radiation per day is in competition with the maximum concentration factor. Thus, the reflector can be modified and optimized accordingly.

III. RADIATION BALANCE

The incoming solar radiation is approximated by an ideal Planck-radiation curve with a temperature of 5800 K. According to the previously computed concentration factor an enhanced irradiance of multiple of 1000 W/m ^{2} hit the absorber surface. An idealized selective absorber coating was considered, representing typical state-of-the-art materials. In Fig. 3 this idealized selective absorber spectra with a crossover wavelength of 2 µm is compared to commercial selective absorber spectra [10].

The dominating loss mechanism at elevated temperatures in vacuum tubes is thermal radiation. We have calculated, at which absorber temperature the absorbed and emitted radiation is balanced depending on the extracted heat. Fig. 4 compares the absorbed radiation spectrum with the emitted radiation spectrum for stagnation, i.e. without any extracted power. The emitted radiation spectrum differs significantly from a thermal radiation spectrum corresponding to the absorber temperature due to the selective absorber.

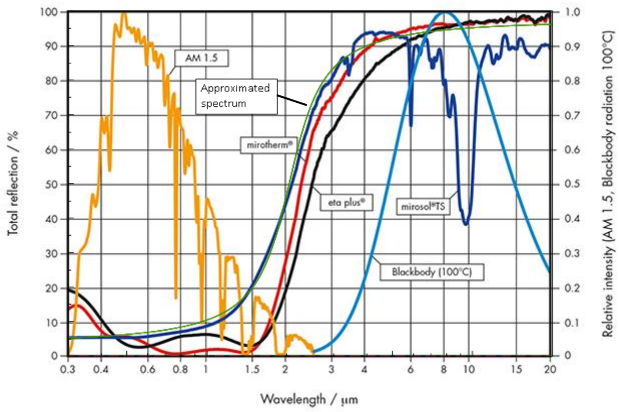

Fig. 3. Typical selective absorber spectra compared to our approximation (green).

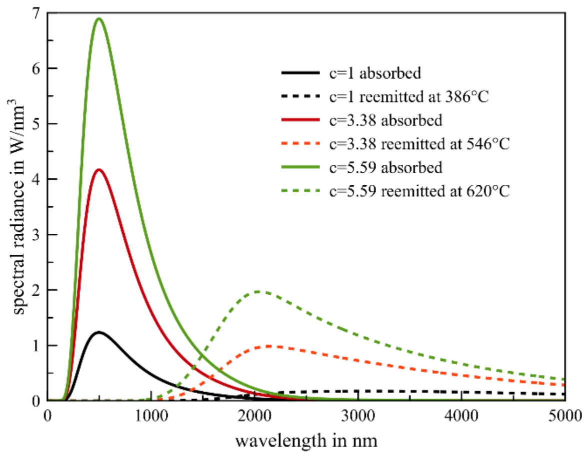

Fig. 4. Radiative heat transfer spectra, balanced using selective absorber in case of stagnation.

With increasing concentration factor the absorber temperature is elevated and the maximum of the thermal radiation shifts towards shorter wavelengths, closer to the crossover wavelength of the selective absorber. The more heat is extracted from the absorbing layer, the lower the absorber temperature. Fig. 5 shows this highly nonlinear relation for different concentration factors.

The conversion of heat into other forms of energy is limited by the Carnot efficiency, which requires maximized temperatures. It is therefore important to optimize the operation point such that the converted heat is maximized. A fraction of the incoming solar radiation is converted into heat, which may be further converted with the Carnot efficiency. This fraction is maximized for a properly chosen temperature as shown in Fig. 6.

It can be seen that an enhanced concentration factor leads to a significant enhancement of the Carnot efficiency at the operation point, where the converted output power is maximized.

The choice of the crossover wavelength of the selective absorber has a weak effect on the absorber temperature. Either the solar irradiation is not fully absorbed or the thermal reemission is not fully blocked. It turned out that for the highest concentration the absorber temperature changed only about 10 K by changing the crossover wavelength in the interval between 2000 nm to 3000 nm, with a maximum at about 2500 nm.

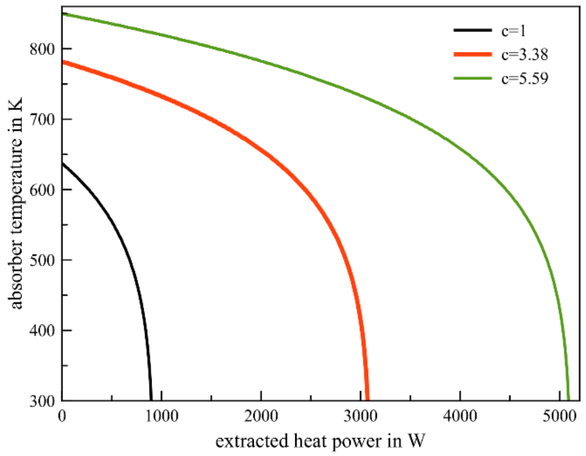

Fig. 5. The resulting absorber temperatures depend on the amount of heat extracted from the system.

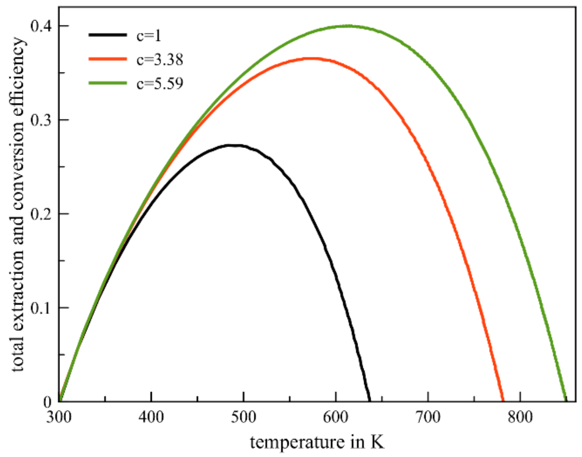

Fig. 6. The heat that is extracted and converted has to be maximized.

IV. Implementations

Our calculations are based on several simplifications and approximations, such that the predicted performance cannot be fully achieved in real systems. However, a careful system design will get close to the computed efficiencies. The main challenges are the precision of the reflector alignment and its reflectivity properties as well as additional heat losses within pipelines.

Vacuum tubes are equipped with a metallic getter material to maintain low pressures, which is highly reflective, but not used for any optical purposes. We suggest shaping the glass wall of the tubes and coating a fraction of the total inner surface with getter material in order to form the computed optimized reflectors inside of the tube. This will not only maintain the vacuum during a longer lifetime, but also avoid all alignment problems as well as reflector corrosion and contamination. While it might be very challenging to shape the most common double-walled (Sydney) tubes, single walled vacuum tubes [11] could be deformed in a single process.

In order to minimize additional heat losses, good vacuum as well as shortest pipelines are required. Therefore, we take a closer look at local and scalable conversion technologies rather than one single conversion system connected to a heat storage tank. Technologies like thermoacoustic, thermomagnetic, or organic rankine [12] are suitable to convert heat with reasonable efficiency at the predicted temperature levels. However, only thermoelectric (TE) components are scalable and allow a heat conversion at each single vacuum tube directly between the absorber and a common water pipeline cooling. Based on the characteristic figure-of-merit of thermoelectric materials ZT, the total conversion efficiency from heat into electricity can be calculated with the hot and cold side temperatures T_H and T_C, respectively:

$$\eta_{tot} = \eta_{tot} \cdot \frac{\sqrt{1+ZT}-1}{\sqrt{1+ZT}+\frac{T_C}{T_H}} \tag{3}$$

Commercially available thermoelectric modules still operate in the ZT range of about 1, whereas the operation temperature can be as high as 800 ℃ [13]. Apart from bulk TE-modules, flexible thick-film geometries are promising candidates [14], which can be directly connected to absorber plates. Embedding those TE-modules into the vacuum tube is very beneficial as a perfect sealing against corrosion and degradation.

Depending on the concentration factor, we can predict the Carnot efficiency, the thermoelectric conversion efficiency and the electric output power density. In Table II the parameters are summarized based on a solar irradiation of 1000 W/m ²and a cold side temperature of 300 K.

TABLE II: Comparison of Optimized System Performance

Concen-tration factor	Extracted power in W	Absorber temp in K	Carnot efficiency	TE efficiency	Power density in W/m ²
1	720	483	37.9%	7.7%	55.4
3.38	2610	569	47.2%	10.1%	41.2
5.59	4560	583	48.5%	10.4%	74.1

The maximum system efficiency is given by the extracted and converted heat (according to Fig. 6 and equation 3) compared to the solar irradiance: 474 W / 5590 W = 8.4% can now be compared to alternative technologies like PV. The electrical output efficiency alone is not competitive with standard PV systems, but the heat efficiency has to be taken into account as well, which is (4560 W – 474 W) / 5590 W = 73.1%. A meaningful operation of such systems should therefore consider the additional cost per power, which can be as low as 0.1 €/W depending on the thermoelectric materials and geometries used. Furthermore, if heat storage systems are connected, they can power the thermoelectric conversion at any time independent from the current solar radiation. The very low cost of heat storages as compared to electric energy storages makes this approach very promising.

In addition to cogeneration of heat and electricity, any measure to enhance the absorber temperature is highly desirable. Solar cooling and solar process heating systems all require elevated operation temperatures in the range 200 ℃-300 ℃, which can be addressed with the proposed non-tracking concentrator.

V. CONCLUSIONS

We have performed different optimization procedures to evaluate the maximum output performance of a non-tracking solar cogeneration system. Restricted irradiation angles enabled the design of a 2D reflector surface offering an effective annual average concentration factor of 3.38. The spectral analysis of incoming radiation, selective absorber and thermal emission allow the computation of the temperature for different heat power extracted from the system. We predict thermal efficiencies of more than 70% and thermoelectric cogeneration of 10% at an absorber temperature as high as 310 ℃.

REFERENCES

[1] F. Dimroth, M. Grave, P. Beutel *et al.*, "Wafer bonded four-junction GaInP/GaAs//GaInAsP/GaInAs concentrator solar cells with 44.7% efficiency," *Prog. in Photovoltaics*, vol. 22, pp. 277–282, 2014.

[2] M. Antonelli, A. Baccioli, M. Francesconi, R. Lensi, and L. Martorano, "Analysis of a low concentration solar plant with compound parabolic collectors and a rotary expander for electricity generation," *Energy Procedia*, vol. 45, pp. 170-179, 2014.

[3] C. Grass, W. Schoelkopf, L. Staudacher *et al.*, "Comparison of the optics of non-tracking and novel types of tracking solar thermal collectors for process heat applications up to 300 ℃," *Solar Energy*, vol. 76, pp. 207–215, 2004.

[4] J. Muschaweck, W. Spirkl, A. Timinger *et al.*, "Optimized reflectors for non-tracking solar collectors with tubular absorbers," *Solar Energy*, vol. 68, pp. 151–159, 2000.

[5] M. Canaff and W. Ratismith, "High productivity non-tracking solar collectors for process heat applications," in *Proc.* 2015 *IEEE 15th International Conference on Environment and Electrical Engineering (EEEIC)*, Rome, 2015, pp. 343-346

[6] S. A. Mondol, B. Vogel, and G. Bastian, "Large scale water lens for solar concentration," *Optics Express*, vol. 23, p. 692, 2015.

[7] J. J. O'Gallagher, "Nonimaging optics in solar energy," *Synthesis Lectures on Energy and the Environment: Technology, Science, and Society*, vol. 2, no. 1, pp. 1-120 , 2008.

[8] A. B. Meinel and M. P. Meinel, *Applied Solar Energy*, Addison Wesley, Publishing Co., 1976.

[9] What is FRED. [Online]. Available: http://photonengr.com/fred-software/

[10] Absorption Products – Particularly Absorbent. [Online]. Available: http://www.alanod-solar.com/en/Absorption/Products

[11] STC – Single Tube Collector. [Online]. Available: http://akotec.eu/en/products/collectors/stc-single-tube-collector/

[12] P. Gang, L. Jing, and J. Jie, "Analysis of low temperature solar thermal electric generation using regenerative Organic Rankine Cycle", *Applied Thermal Engineering*, vol. 30, pp. 998–1004, 2010.

[13] [Online]. Available: http://www.toshiba-tmat.co.jp/eng/res/theme3.htm

[14] A. Heghmanns, M. Beitelschmidt, S. Wilbrecht, K. Geraedts, and G. Span, "Development and optimization of a TEG-system for the waste heat usage in railway vehicles," *Materials Today*, vol. 2, p. 780, 2015.

Georg Bastian studied physics at the Universiy of Duisburg, Duisburg, Germany, and the University of Marburg, Marburg, Germany. He received his diploma degree in semiconductor optics and the Ph.D. degree in quantum electronics at the Physikalisch-Technische Bundesanstalt (PTB) Braunschweig, Germany, in 1995 and 1998, respetively.

In 1999 he joined the NTT Basic Research Laboratories, Atsugi, Japan, investigating cavities for Cooper-pairs. In 2000, he was involved in current standards using surface acoustic waves at the PTB, before moving to Alcatel SEL, Stuttgart, Germany, where he was responsible for research on photonic crystals until 2002. He became the CTO of the Institute for Light Technology, University of Karlsruhe, Karlsruhe, Germany, working on nanotechnology and optoelectronics. From 2006 until 2010, he has been working as a professor at the University of Applied Science, Trier, Germany. In 2010 he joined the Rhein-Waal University of Applied Sciences in Kleve, Germany, working on applied optical systems and renewable energy.